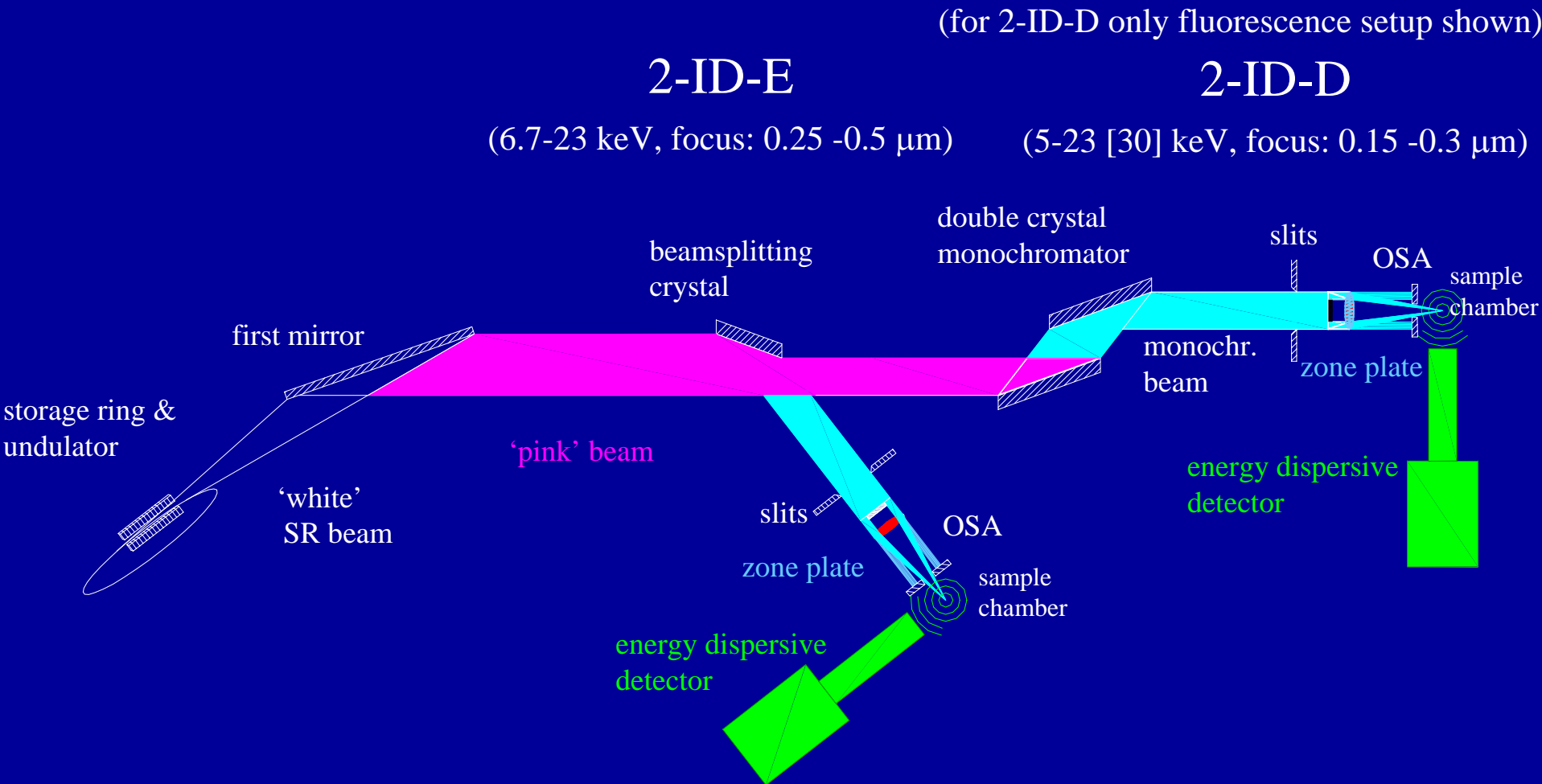


# INTRODUCTION: Biological Applications of X-ray Microprobe

Gayle E. Woloschak  
Northwestern University

# 2-ID-D/E hard X-ray microprobe beamline at the APS



- image sample by raster scanning the sample through focused beam
- acquire & save **full spectra** (simultaneously) at each scan position
- analyze spectra at each scan position

## Workshop on Biological Applications of X-ray Microbeams

Recent studies in cell biology, environmental science, and microbiology using hard X-ray microprobes have yielded promising results. This led to a workshop on existing biological applications, benefits, and future needs of high-resolution X-ray microscopy. About 50 researchers attended the workshop held May 14-15, 2001, at Argonne National Laboratory.

Hard X-ray microprobes have been used for several years (Fig. 1) [1]. Broadly speaking, the applications can be classified as analyses of tissues, eukaryotic cells and microorganisms. The high elemental sensitivity of X-ray fluorescence and the high spatial resolution offered by the X-ray microprobe are crucial for trace-element mapping and analysis in these systems. Current applications include medical studies in the areas of pathogenesis, carcinogenesis, and drug efficiency, and environmental studies in marine biology and geo-microbiology. Examples include cellular investigations that address elemental imaging of cells for drug metabolism (P and S), metal metabolism (Cu and Zn), trace-metal concentrations in cells, and elements from mineral surfaces, and trace metals in marine and freshwater microbes, and cellular processes, such as changes in metal distribution during differentiation, cell cycle progression, etc. Several groups are labeling cellular and subcellular structures with antibodies bound to metals or with Tl<sub>20</sub> nanoparticles with bound DNA or peptides. Expansion of these approaches to other metals would increase the number of intracellular structures that could be resolved. A noncellular use of the hard X-ray microprobe is microtomography, which has been used to study bone ultrastructural changes. Soft X-ray tomography has already led to 3D imaging of cryogenic specimens providing intracellular structures of single cell preparations and some cellular substructures (such as nuclei, nucleoli, and others).

These types of studies, as well as classic biological applications, which are predominantly observation of natural events, will



May 14-15, 2001

also been found in some patients with Alzheimer's and Parkinson disease [3]. Calcium and zinc-permeable receptor channels were implicated in selective neurodegeneration in cases of global ischemia, Alzheimer's disease, and amyotrophic lateral sclerosis [4]. Hard X-ray elemental mapping and spectroscopy is likely to shed some light on the role of metals in the pathogenesis and progression of these diseases and may also permit imaging of the intracellular inclusions caused from metal-binding proteins. Finally, recent studies have demonstrated that many oncogenes (genes that become dysregulated in cancer) encode proteins that are transcription factors that bind Zn or cadmium proteins that bind other metals [5]. Hard X-ray elemental mapping with improved resolution will permit new studies of the role of metal binding on the intracellular function of these important proteins and may also permit measuring of intracellular concentration of these proteins.

These types of studies, as well as classic biological applications, which are predominantly observation of natural events, will

## Workshop on Biological Applications of X-ray Microscopy and Imaging

G. Bilekchuk (Northwestern University),  
B. Liu (Argonne National Laboratory),  
J. Mayer (Argonne National Laboratory),  
S. Rigi (Argonne National Laboratory),  
Z. Hamada (Northwestern University)

A workshop on the biological applications of X-ray microscopy and imaging was held in conjunction with the 12th Users Meeting for the APS. The workshop was hosted jointly by the APS and Northwestern University Medical Center and was the second workshop designed to discuss current capabilities and future developments of X-ray microscopy and to identify novel applications. Presentations from 17 speakers from around the globe and a conference summary (presented by Peter Ijzerman, Duke University Medical Center) provided the focal point for discussion at the workshop. A variety of different approaches to imaging were highlighted at the workshop, including current capabilities in fluorescence, spectroscopic and imaging approaches for visualization of processes occurring at the subcellular, cellular, and whole-animal levels.

Speakers from different institutions presented lectures on state-of-the-art applications of electron microscopy, optical microscopy, microCT, diffraction-enhanced imaging, and MRI to provide a context for X-ray microscopy-based imaging approaches. Several lectures were devoted to a description of ongoing studies using X-ray microscopy at the APS at Argonne National Laboratory, National Synchrotron Light Source at Brookhaven National Laboratory, European Synchrotron Radiation Facility, and other sites. Applications discussed in detail included studies of metal content in bacteria and marine proteins, intracellular metal distribution in mammalian cells, use of X-ray fluorescence for detection of platinum-based anticancer drugs, intracellular probes labeled with Tl<sub>20</sub> nanoparticles, iron in liver tissues from haemochromatosis patients, and iron acquisition of pathogenic mycobacteria.

Applications of X-ray fluorescence to studies of human disease states including forensic medicine, disease pathology, and disease diagnosis were described. The participants noted that other applications of X-ray microscopy are likely but have not yet been explored in the biomedical community.

Much discussion at the workshop centered on possible improvements to existing facilities that could enhance experimental results, and open up new research areas. Since the last workshop (held in 2001), improvements in data management (particularly with regard to statistical applications), communication of results, phase-contrast imaging, and fast-freezing techniques have been made. Nevertheless, several areas of investigation were targeted as being important for future studies including higher spatial resolution, probing cryogenically preserved specimens, elemental microtomography, quantitative structural imaging, and quantitative compositional analysis.

The workshop was generally exciting and successful and the participants agreed on the need for holding similar workshops in future APS users meetings.



Discussion during the coffee break of the Workshop on the Biological Applications of X-ray Microscopy and Imaging.

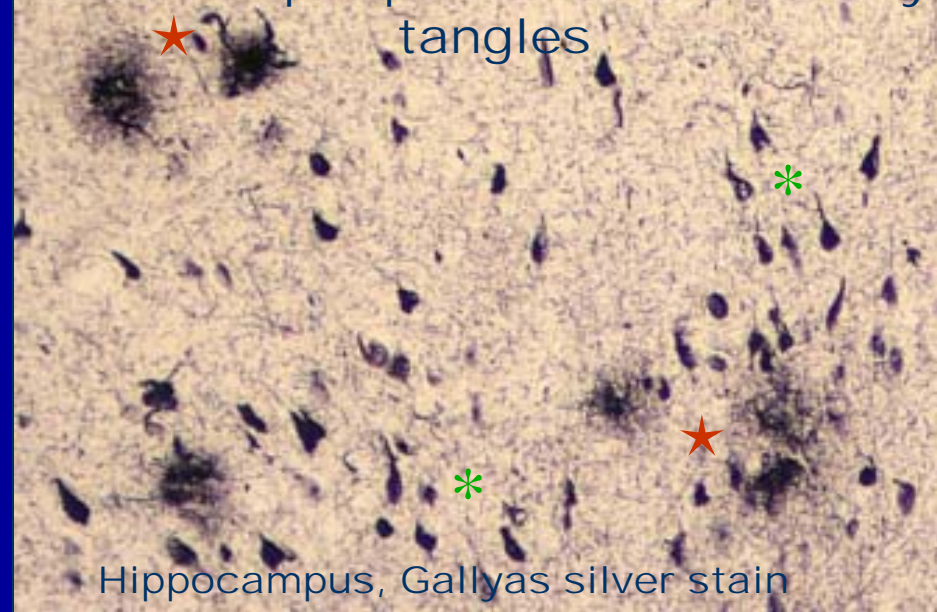
# Biological Applications of X-ray Microprobe

- Microbial analyses
- Environmental studies
- Metal toxicity/Carcinogenesis/Cancer
- Chemotherapeutic drugs
- Infectious parasites/Anti-parasitic drugs
- Neurologic diseases
- Nanobiotechnology

- **Alzheimer disease**

- Related to beta amyloid (Abeta<sub>42</sub>) protein/oligomers deposition
- Amyloid precursor protein regulates Cu homeostasis
- Pathology
  - Neurofibrillary tangles (tau protein) \*
  - Neuritic plaques (tau & Abeta) ★
- Metal-protein-attenuation therapy improves cognition & lowers serum Abeta<sub>42</sub> (*Arch. Neurol.* 2003;60:1685-91)

Neuritic plaques & neurofibrillary tangles



Hippocampus, Gallyas silver stain

- **Lewy body diseases**

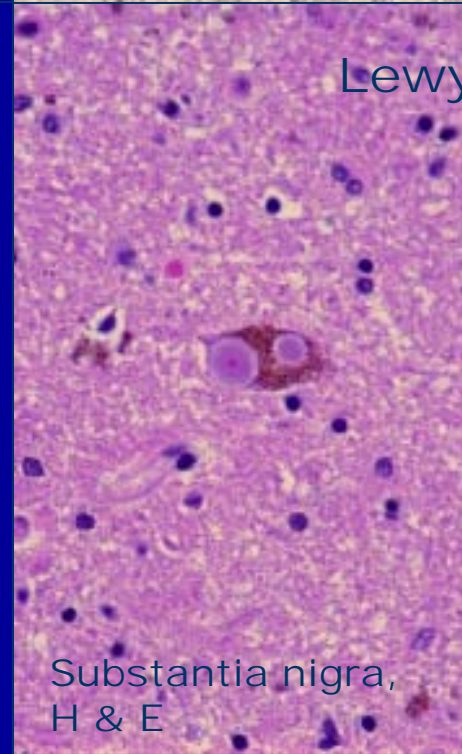
- **Pathology**

- Lewy bodies in brainstem (Parkinson disease)
- Lewy bodies in brainstem and cortex (Dementia with Lewy bodies)

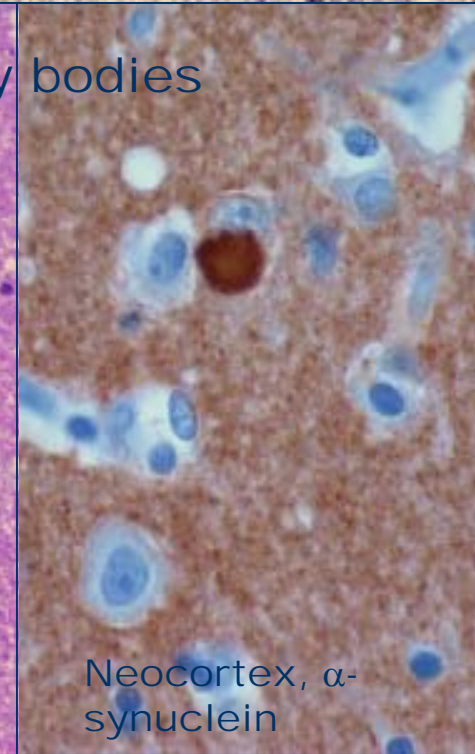
- **Lewy bodies**

- Composed of aggregated  $\alpha$ -synuclein, pre-synaptic protein—uncertain function
- Metals (Al, Cu, Fe, Co, Mn) trigger aggregation / fibrillation of alpha-synuclein (*J Biol Chem* 2001;276:44284-96)

Lewy bodies



Substantia nigra,  
H & E



Neocortex,  $\alpha$ -  
synuclein

# Intracellular Manipulation with TiO<sub>2</sub>-DNA Nanocomposites

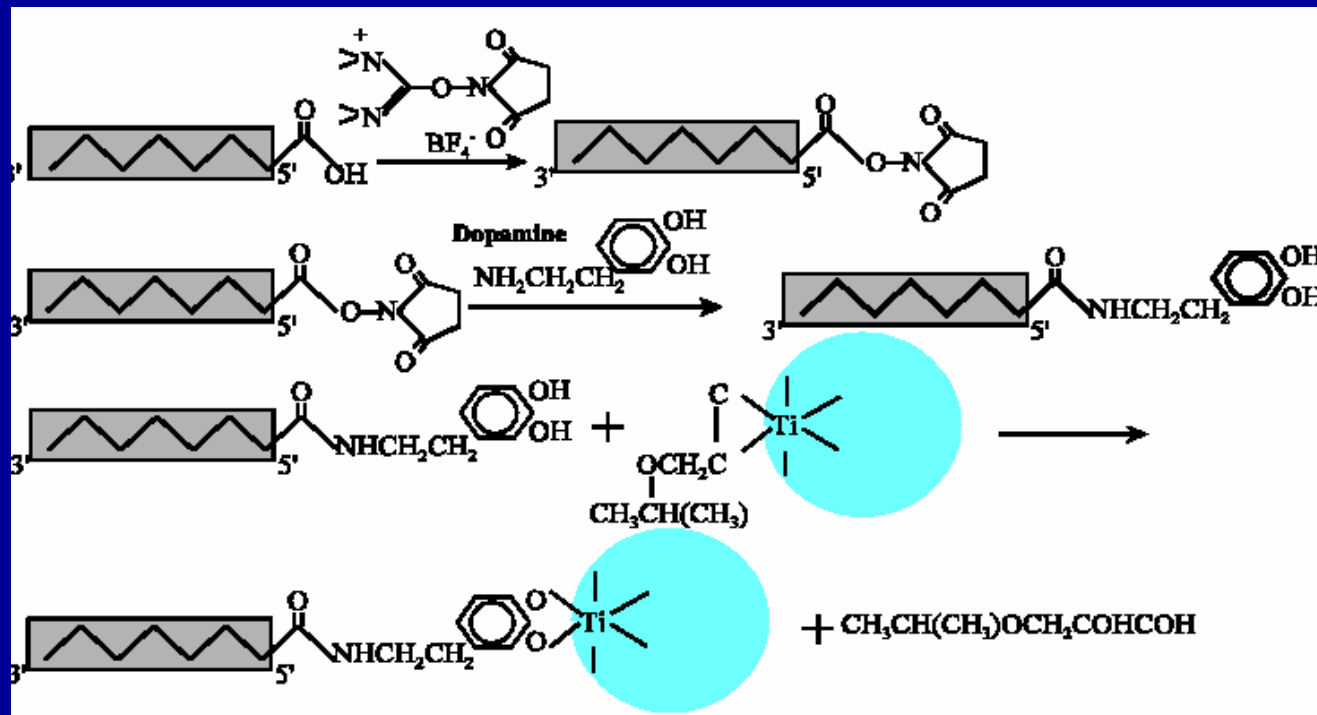
Gayle E. Woloschak  
Northwestern University

# Properties of Titanium Dioxide Nanoparticles

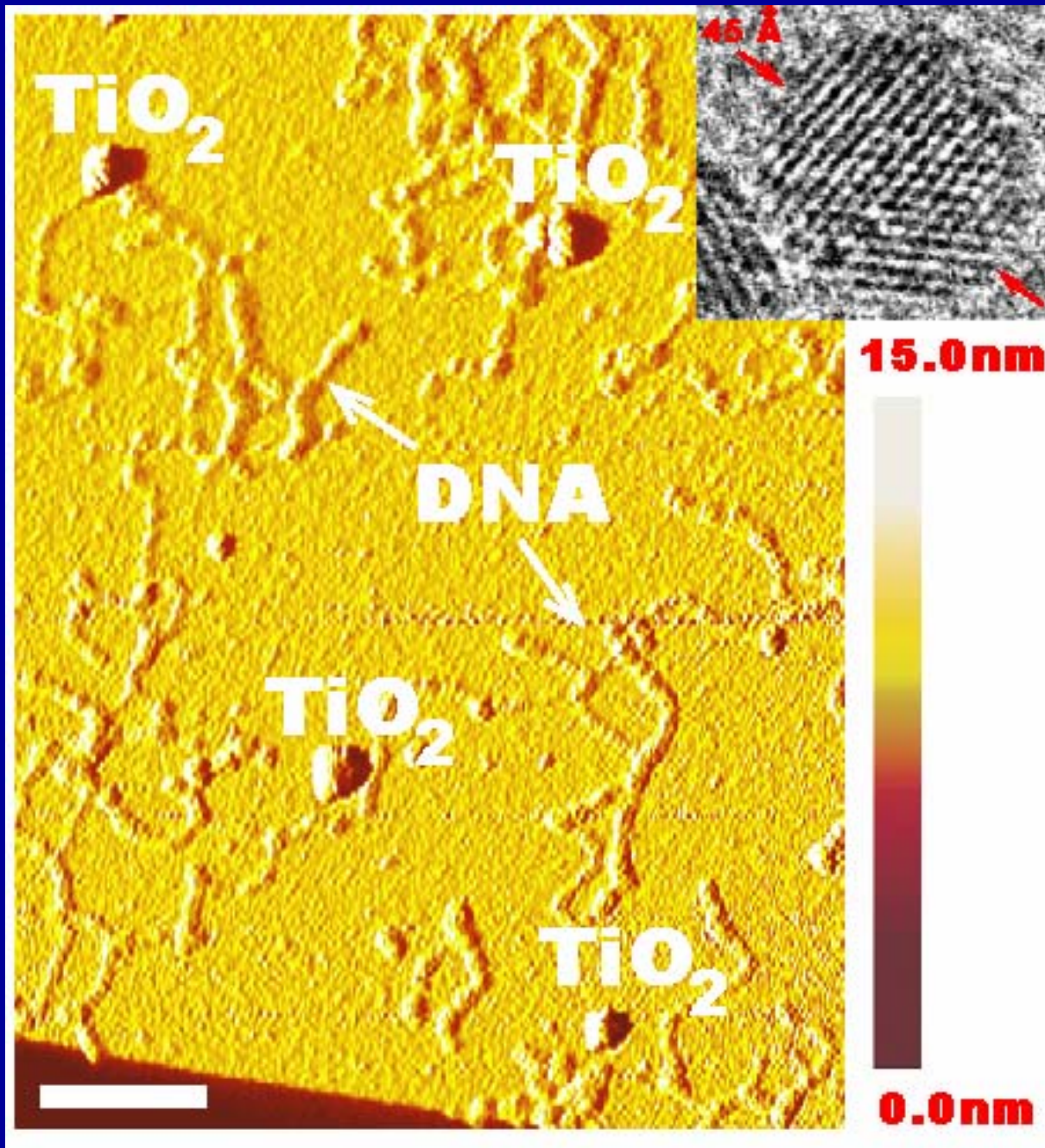
-Smaller than 20 nm— “corner defects” and readily bind modifiers (dopamine)

-Use of organic modifiers—semiconducting through metal oxide and organic modifier

-Charge pairs are separated into electropositive holes on the donating organic modifier and the electrons in the conduction band of  $\text{TiO}_2$



Individual steps for binding of 5' carboxyl group modified oligonucleotides to  $\text{TiO}_2$  nanoparticles using succinimide method. In the first step  $\text{COOH}$  group is bound to O-N-succinimidyl-NNN'N'-tetramethyluronium tetrafluoroborate in the presence of N-N-diisopropylethylenamine. In the second step the succinimidyl complex is replaced with dopamine via terminal amino group. In the third step the dopamine end-labeled oligonucleotide replaces glycidil isopropyl ether modified  $\text{TiO}_2$  nanoparticle due to the higher stability of the dopamine  $\text{TiO}_2$  complex.



**Atomic Force Microscopy image of  $\text{TiO}_2$ -oligonucleotide nanocomposites complementary to the lambda phage DNA following hybridization.**

White scale bar presents 10 microns.

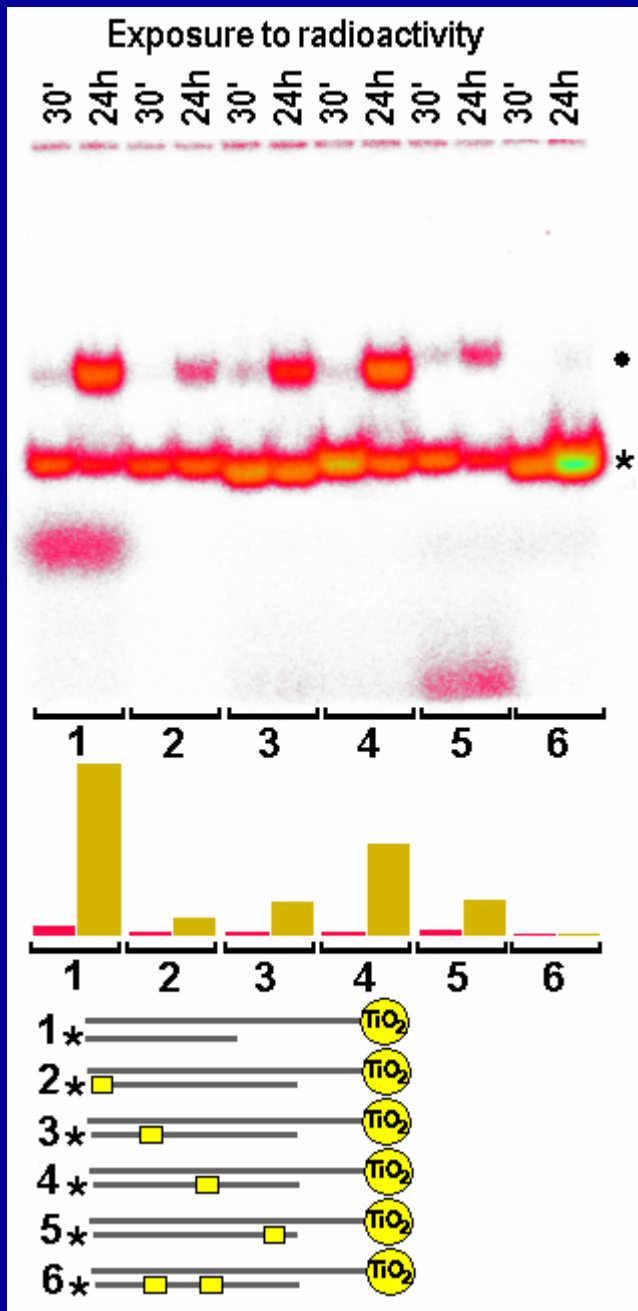
Color gradient presents height.

In the upper right corner is a Transmission Electron Micrograph of a single  $\text{TiO}_2$  particle showing its size (45 Å).

# Properties of TiO<sub>2</sub>-DNA Nanoparticles

- Light- and radiation-induced DNA (and RNA) cleavage that is sequence-specific
- Ability to participate in enzymatic reactions (PCR)
- Subcellular localization (mitochondria, nucleoli)



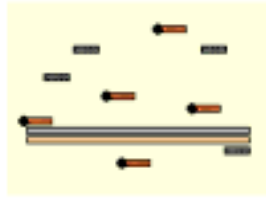


Presence of **mismatches** in the sequence of the oligonucleotide annealing to the  $\text{TiO}_2$ -DNA nanocomposite influences the yield of DNA cleaved from the nanocomposite.

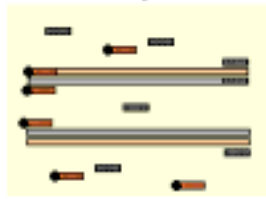
All wells contain a  $\text{TiO}_2/50$  nanocomposite annealed to a full match radiolabeled complementary distal 30-mer (well group 1) different mutated distal 30-mers (well groups 2-5) containing each a set of four consecutive mutated bases, or two sets of four mutated bases (well group 6).

## PCR Experiments

PCR



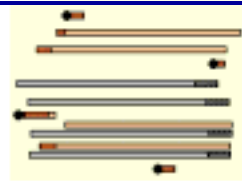
PCR



Mixture of ss and ds PCR product

Gel Electrophoresis

Light



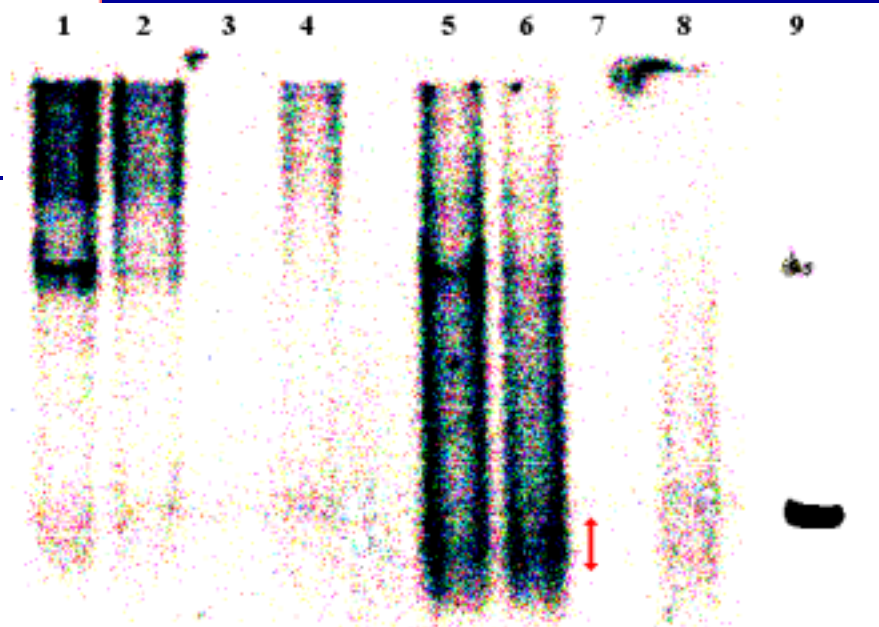
Mixture of ss and ds PCR product and free nanoparticles

Gel Electrophoresis

Negative control: template DNA sequence not matching primers

Positive control: Both primers (oligonucleotides) not bound to TiO<sub>2</sub> nanoparticles

**Illuminated titanium dioxide cuts the attached DNA synthesized by polymerase chain reaction.**



1, 2, 3, 4 = Non-illuminated PCR

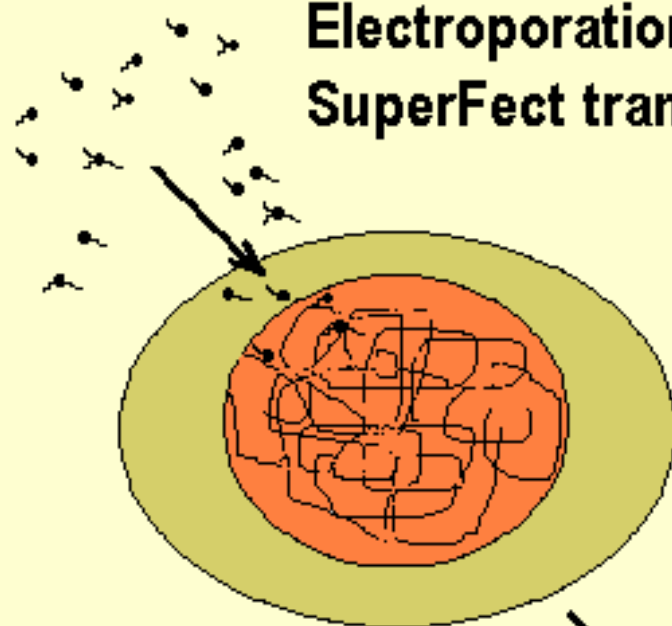
5, 6, 7, 8 = Illuminated PCR

3, 7 = Negative control PCR

9 = Positive control PCR (short exposure)

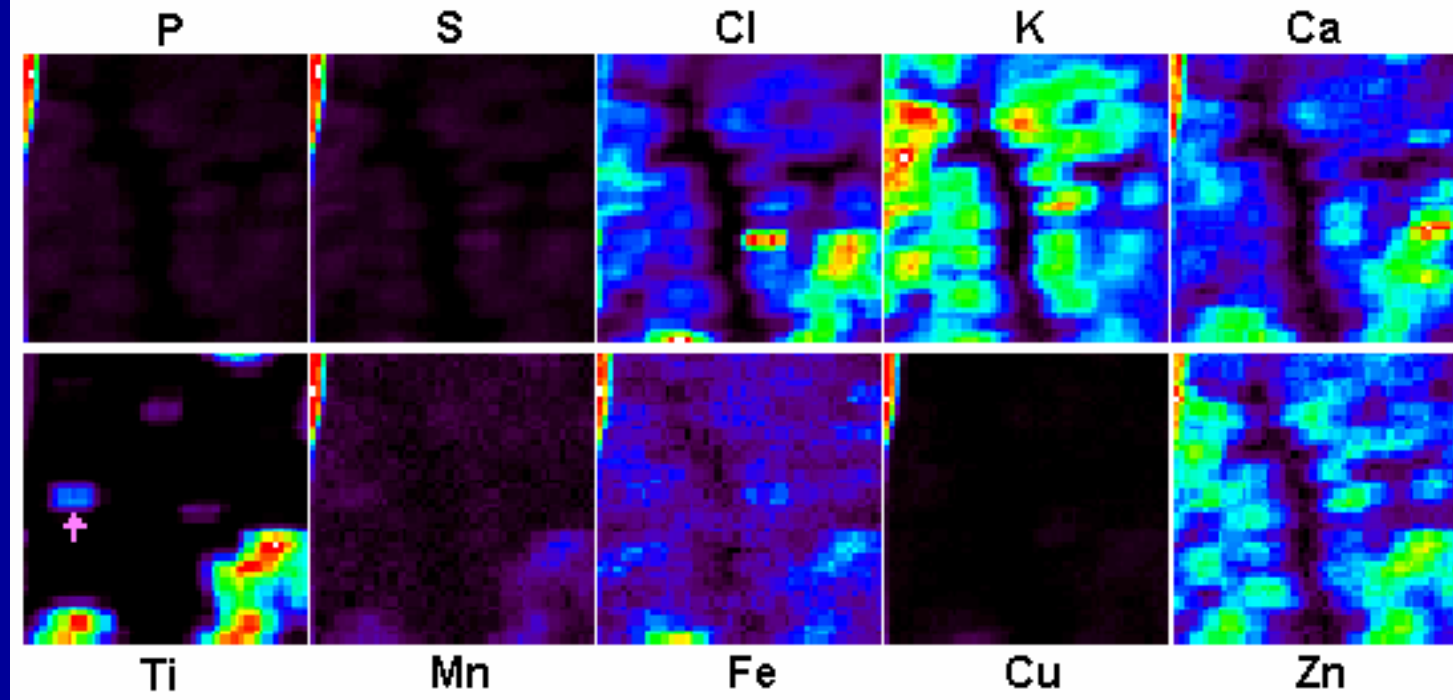
# APS Experiments

Electroporation  
SuperFect transfection



incubation 2-9h

detection of  $K_{\alpha}$  X-ray fluorescence



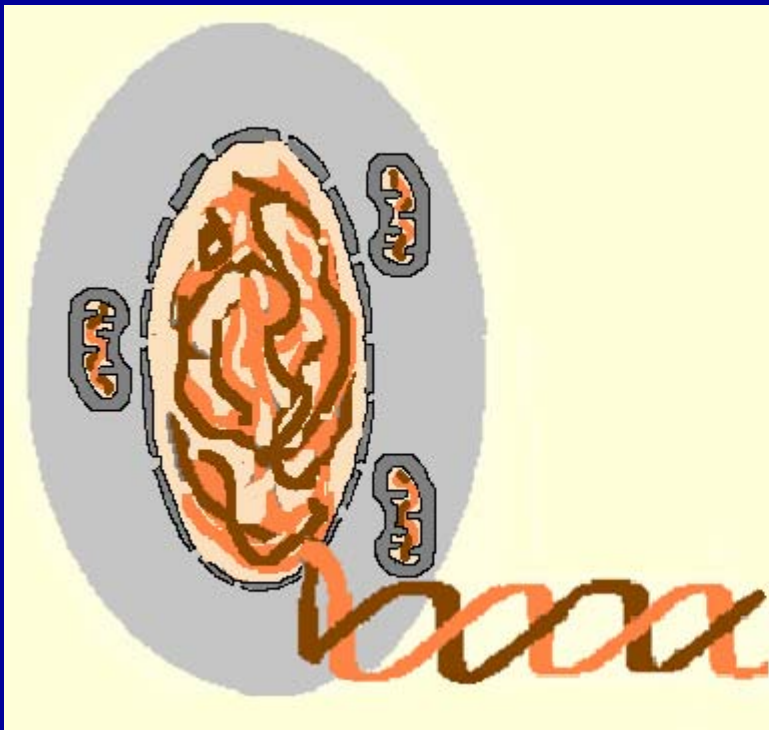
Element distribution maps of P, S, Cl, K, Ca, Ti, Mn, Fe, Cu, and Zn in a scan of a 90 x 90 μm area (in 2 x 2 μm pixels) containing twenty-eight HL60 cells transfected with Ti nanoparticles bound to the oligonucleotide complementary to the 18S rDNA (80 pmol of R18Ss - TiO<sub>2</sub> nanocomposites was added to 2 x 10<sup>6</sup> cells and incubated for two hours).

The map of Ti distribution in this specimen section shows that eight cells contain titanium as a consequence of transfection. One such cell indicated by a pink arrow contains a total of 2.9 x 10<sup>7</sup> TiO<sub>2</sub> nanoparticles (each nanoparticle contains 1400 Ti atoms).

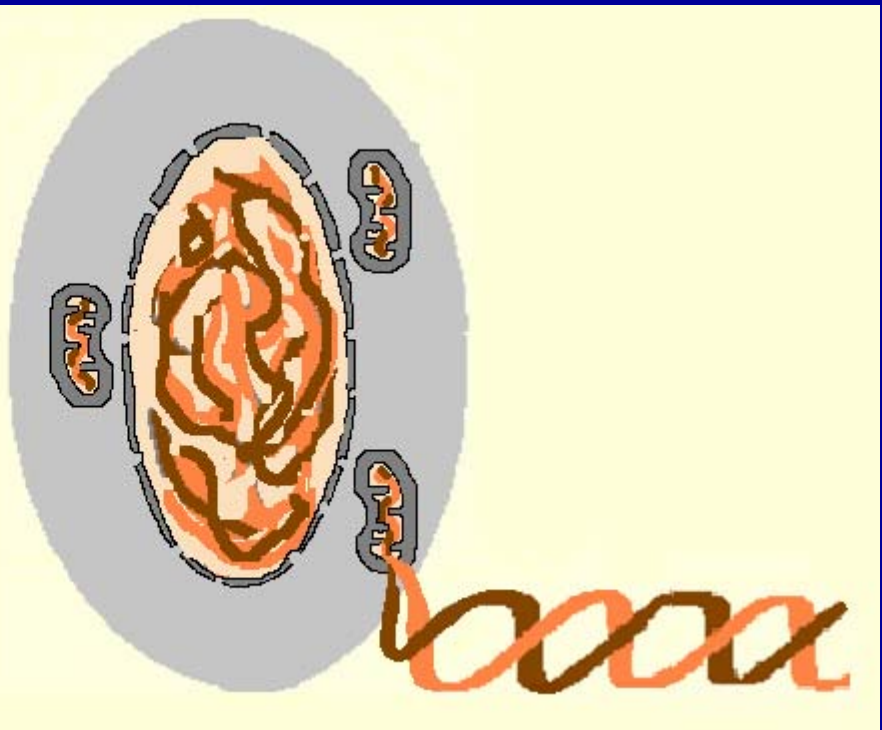
# HYPOTHESIS

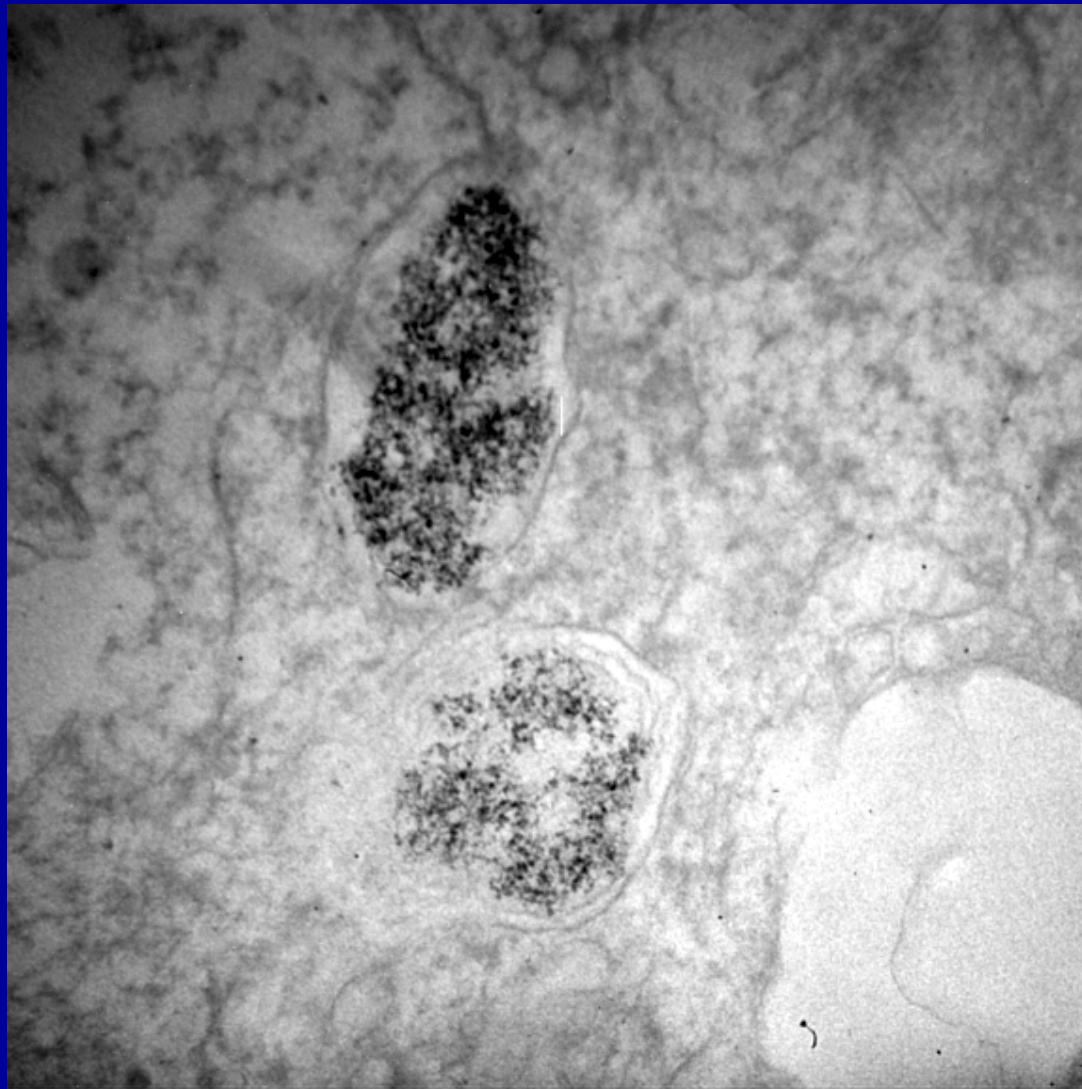
TiO<sub>2</sub> nanocomposites with attached specific DNA sequence should be retained in those locations inside the cell where complementary cellular DNA sequence is located.

## Nuclear DNA



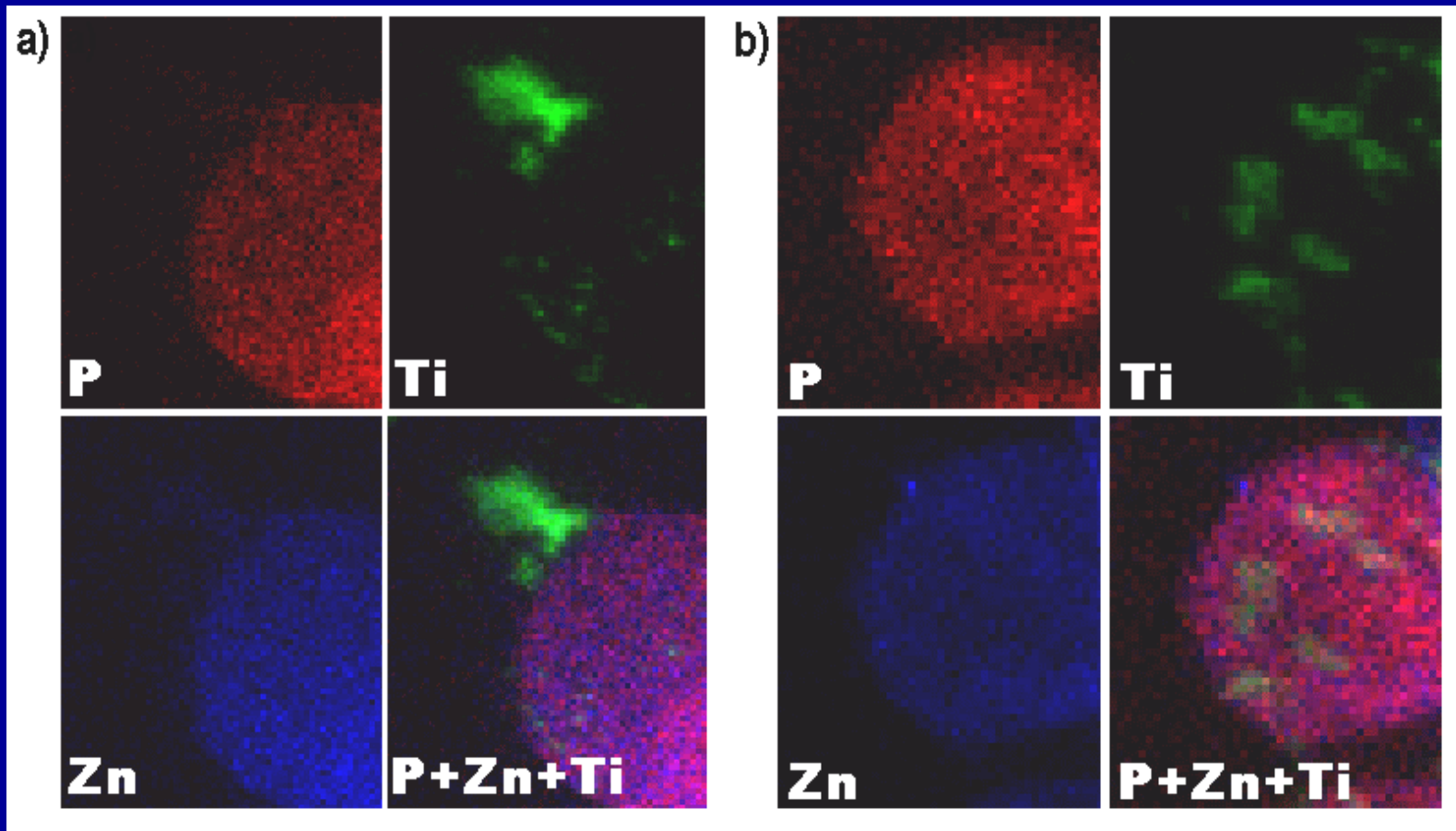
## Mitochondrial DNA





File Name = M1 MIT1.tif  
M1 CELL 1 MITOCHONDRIA A  
Print Mag = 0x @ 0 mm  
Acquired Nov 7 2003 at 4:31 PM  
TEM Mode =

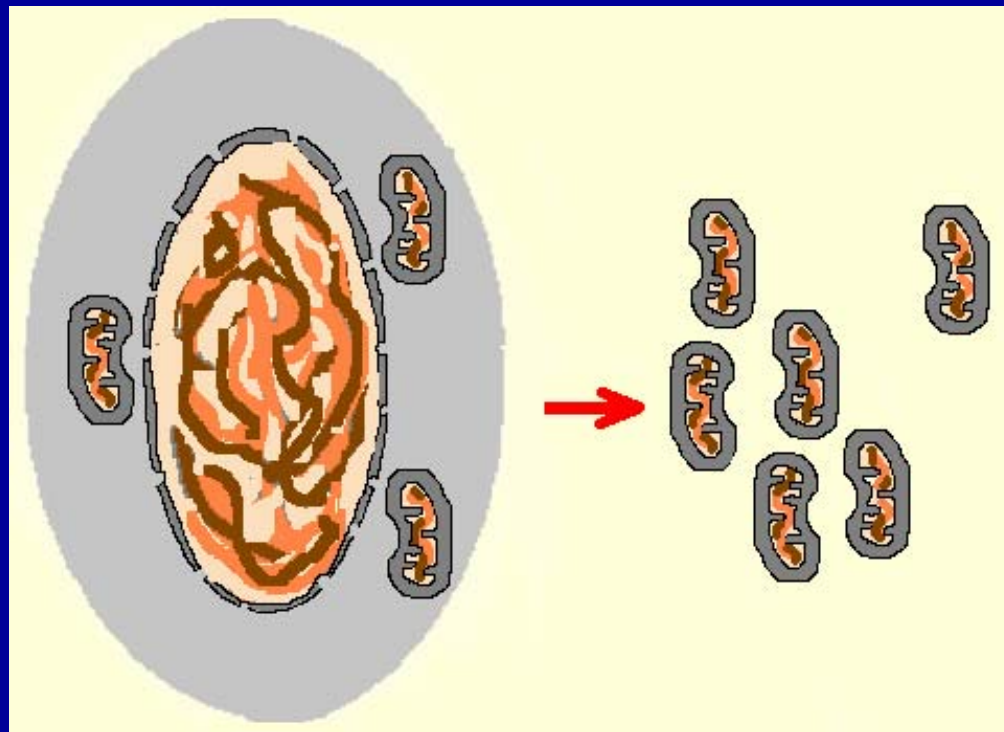
100 nm  
HV=60kV  
TEM Mag = 80000x  
AMT Preferred Customer

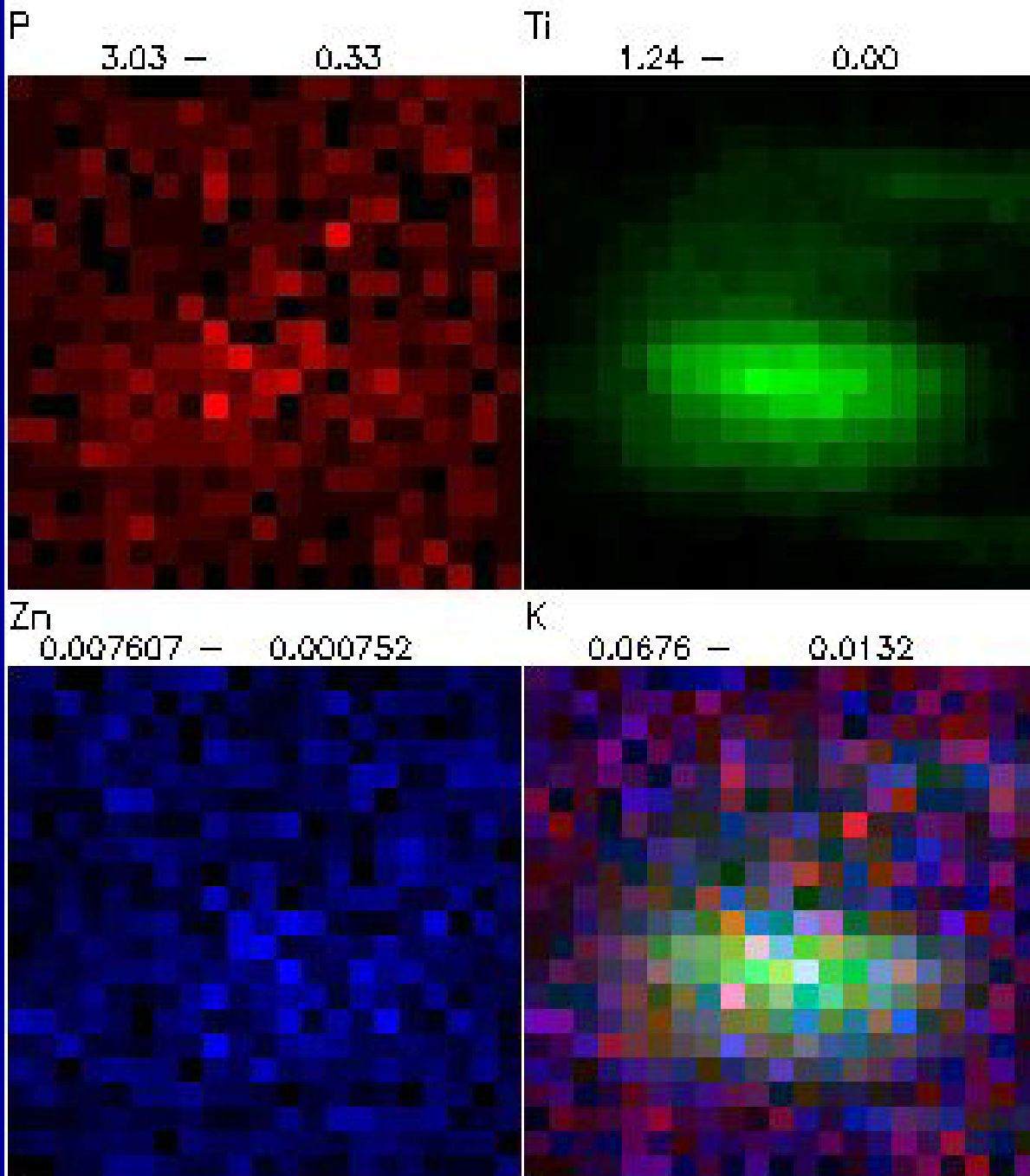


Comparison of phosphorus, zinc, and titanium signals, and their overlap, in a) cell transfected with “free” TiO<sub>2</sub> (left four panels) and b) cell transfected with a combination of TiO<sub>2</sub>-DNA nanocomposites MIT1s-TiO<sub>2</sub> and MIT2s-TiO<sub>2</sub> (right four panels).

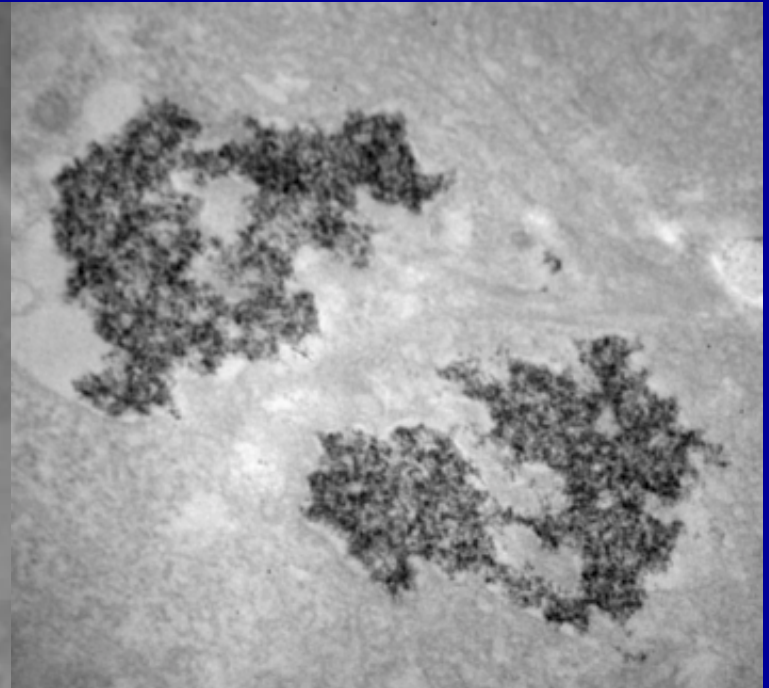
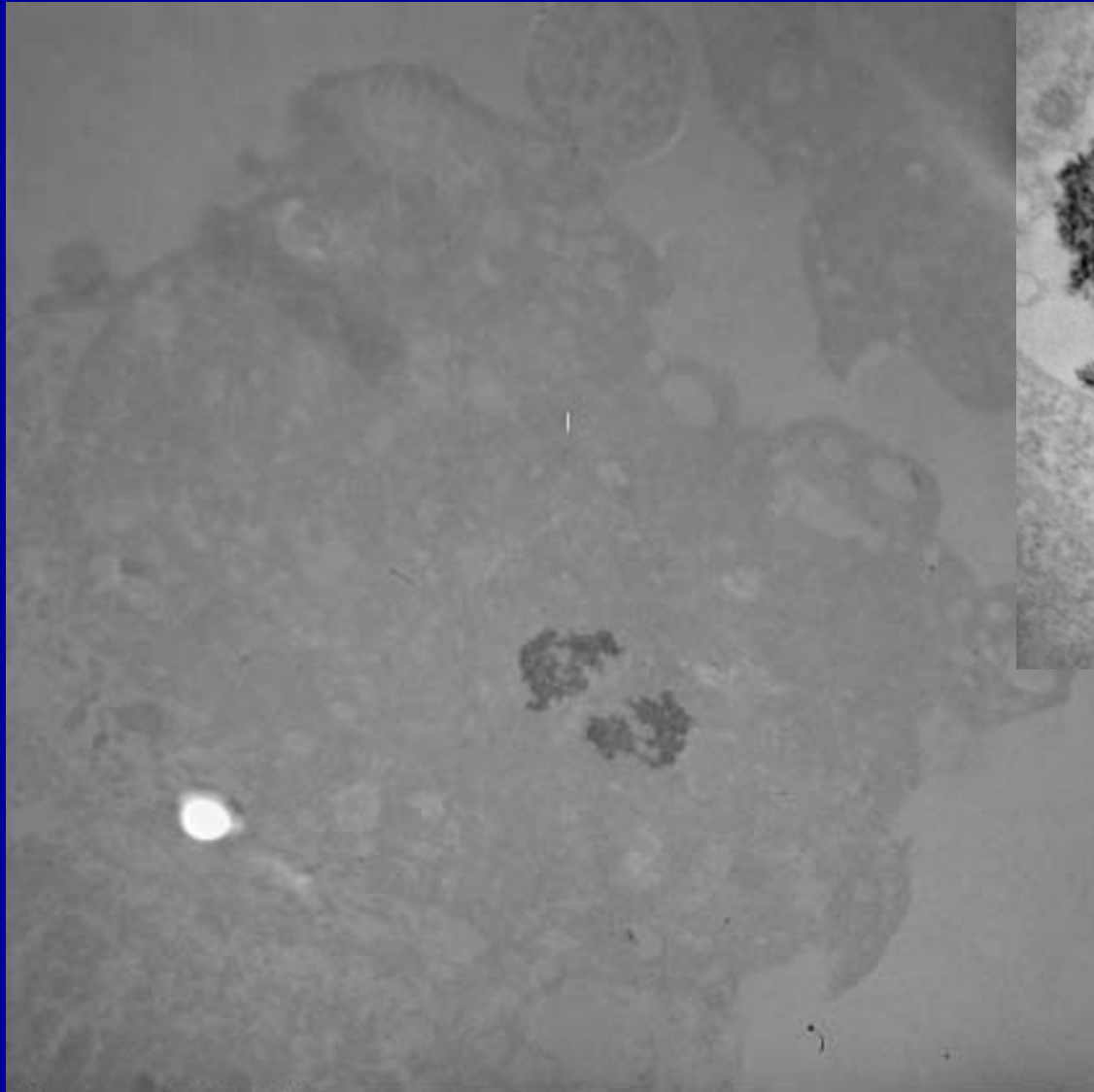
PC12 cells were transfected with a combination of nanoparticles/nanocomposites for 4 hours, washed for 2 hours, detached from the Petri dish, and transferred onto formvar coated EM grids, fixed, dried and scanned.

Individual mitochondria were isolated from PC-12 cells transfected by the “mitochondrion-specific” nanocomposites and applied onto EM grids for visualization at 2-ID-E beamline of XOR-CAT at the APS.





X-ray fluorescence maps (linear scale) of the elements P, Ti and Zn and overlapping image (K) show that the Ti signal is in the mitochondria.



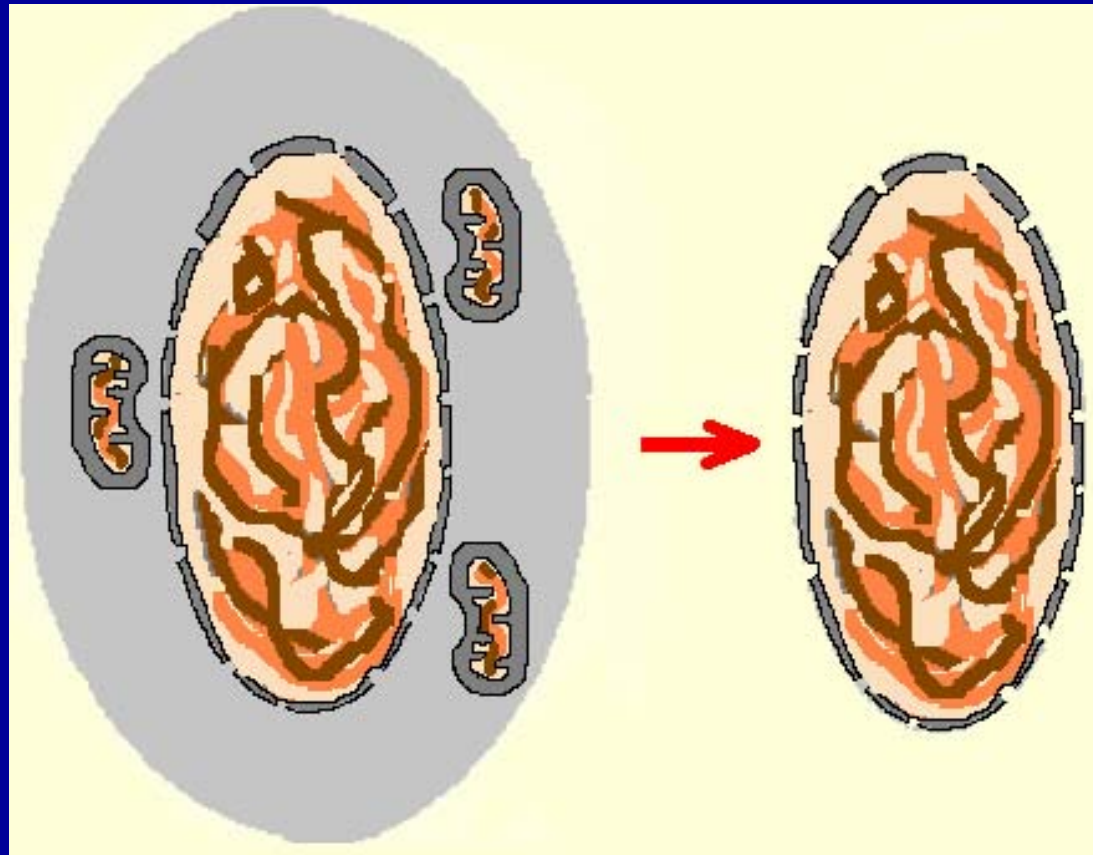
File Name = MCF7 OVW.tif  
MCF7 CELL 1 OVERVIEW  
Print Mag = 0x @ 0 mm  
Acquired Nov 7 2003 at 5:01 PM  
TEM Mode =

2 microns  
HV=60kV  
TEM Mag = 12000x  
AMT Preferred Customer

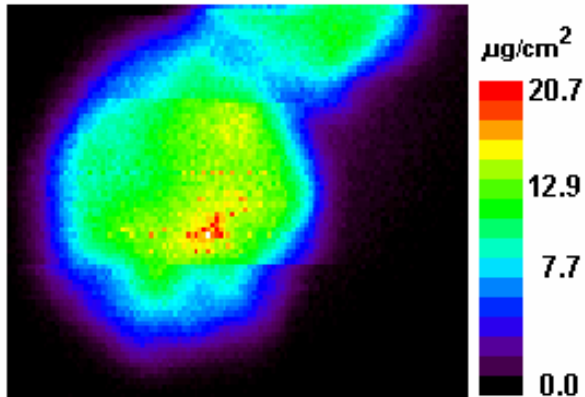
EM image of the MCF-7 cell showing presence of nanocomposites on two locations in the nucleus.

Image obtained at Northwestern Cell Imaging Facility

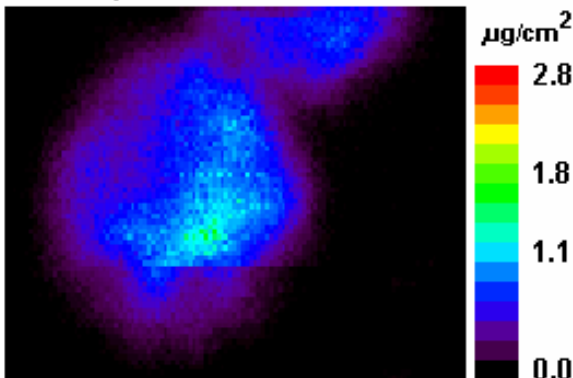
Individual nuclei were isolated from PC-12 cells transfected by the “nucleolus-specific” nanocomposites and applied onto EM grids for visualization at 2-ID-E beamline of XOR-CAT at the APS.



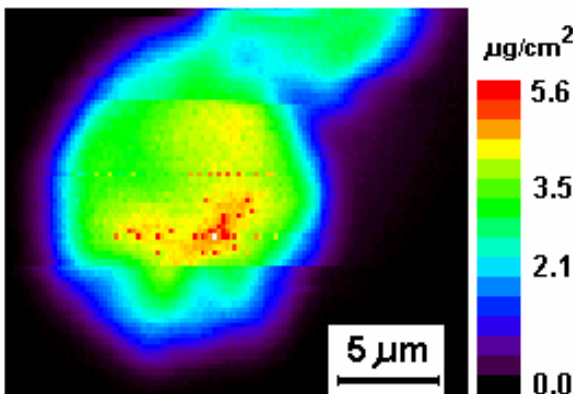
K map



Ti map

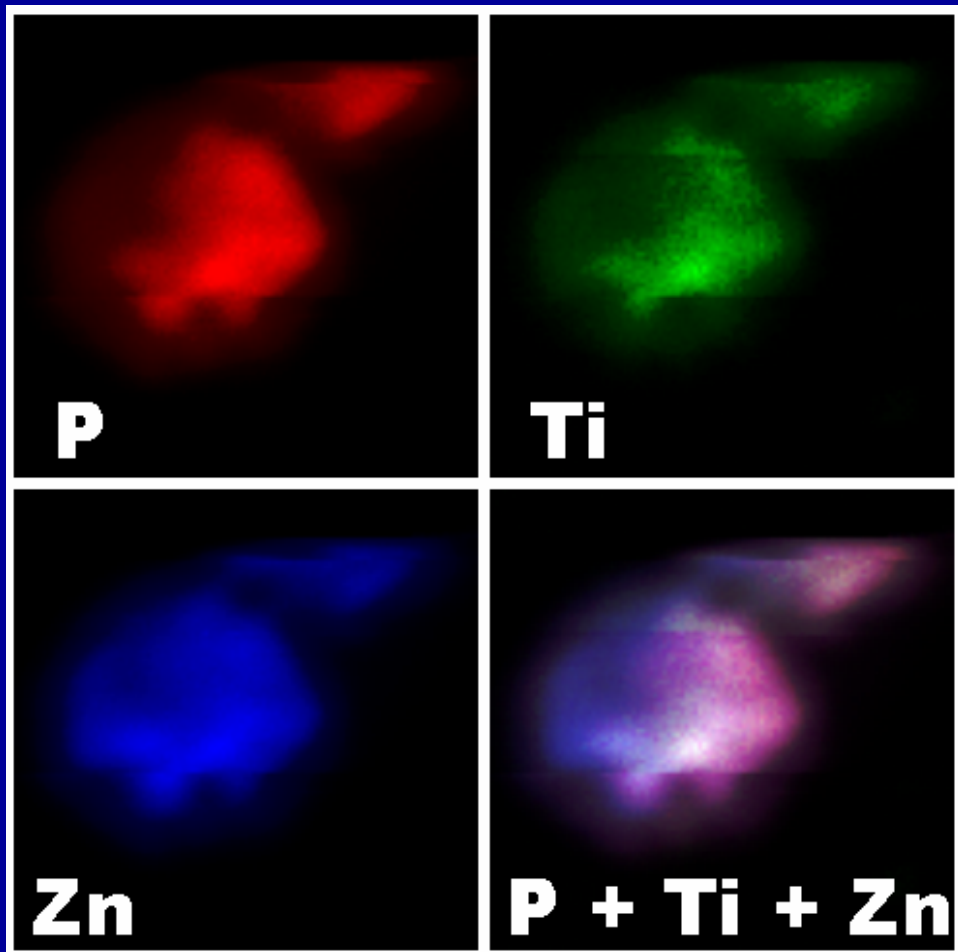


Zn map



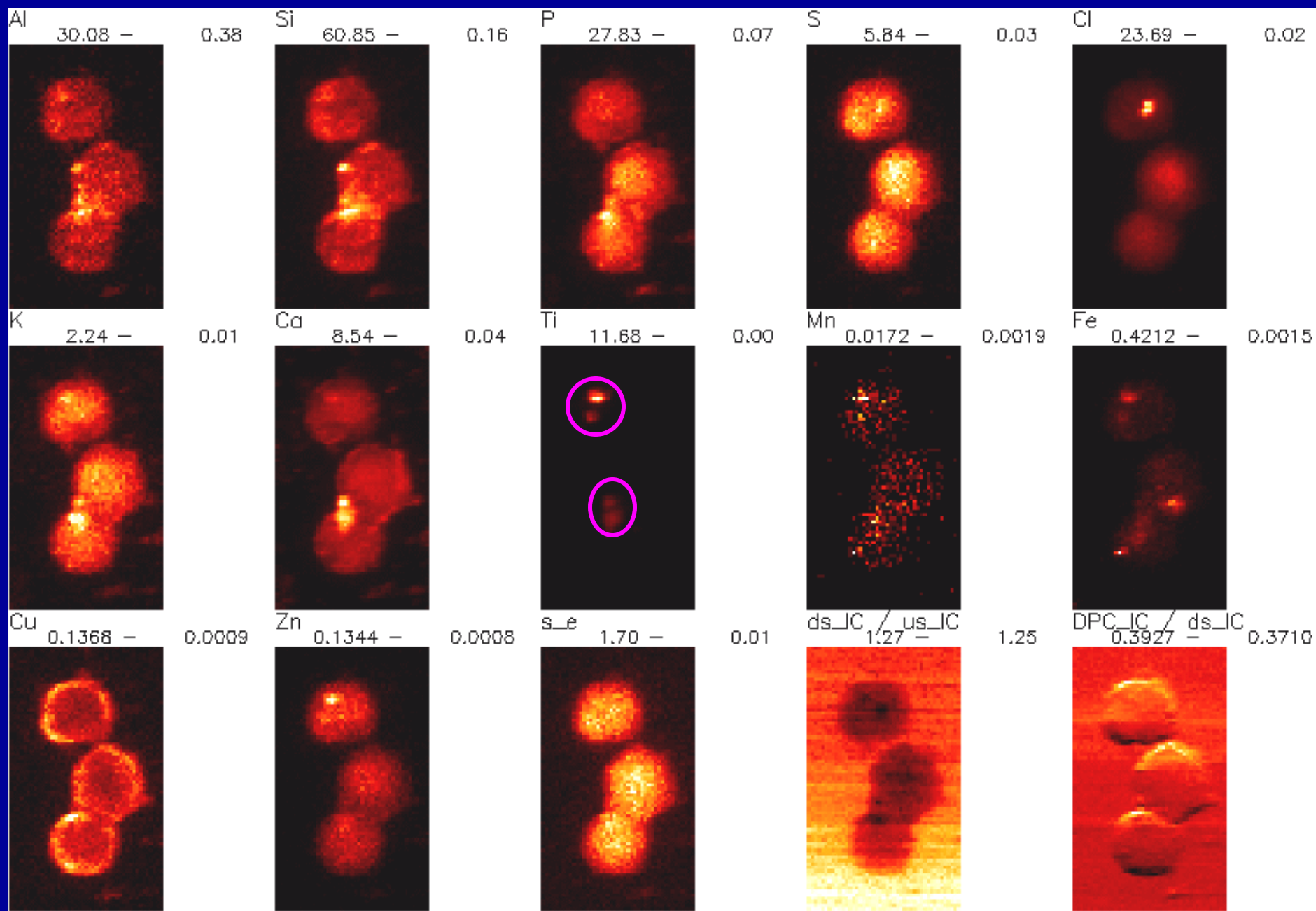
Element distribution maps of K, Ti, and Zn in a single HL60 cell nucleus transfected with nanocomposite complementary to ribosomal DNA (nucleolar DNA).

$0.2\ \mu\text{m} \times 0.2\ \mu\text{m}$  step scan of a single nucleus isolated from HL60 cells following a transfection by SuperFect reagent, with 80 pmol of R18Ss-TiO<sub>2</sub> hybrid nanocomposite, and 160 pmol of “free” R18Sas oligonucleotide applied onto  $4 \times 10^6$  cells incubated for 2 hours.



$K\alpha$  X-ray fluorescence signals of phosphorus, zinc, and titanium, and overlapped with each other, showing the highest titanium signal density in a circular subregion of the nucleus resembling of a nucleus.

Area covered by this scan was  $21 \times 21 \mu\text{m}$  with a single nucleus isolated from HL60 cells transfected with R18Ss-  $\text{TiO}_2$  nanocomposite, and a “free” R18Ss oligonucleotide. By its size and shape this nuclear subregion closely resembles the nucleolus—subregion of the interphase nucleus where rDNA is located, and would therefore be the most likely nuclear location for retention of an R18Ss oligonucleotide activated  $\text{TiO}_2$  nanocomposite. Presumably, such retention would be dependent on hybridization/annealing of R18Ss- $\text{TiO}_2$  nanocomposite with the genomic ribosomal 18S rDNA.



10 μm



MAPS V

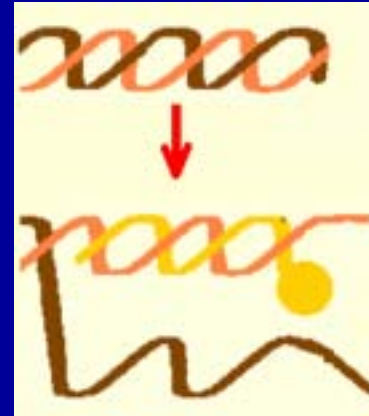
# Properties of TiO<sub>2</sub>-DNA Nanoparticles

- Light- and radiation-induced DNA (and RNA) cleavage that is sequence-specific
- Ability to participate in enzymatic reactions (PCR)
- Subcellular localization (mitochondria, nucleoli)

# HYPOTHESIS

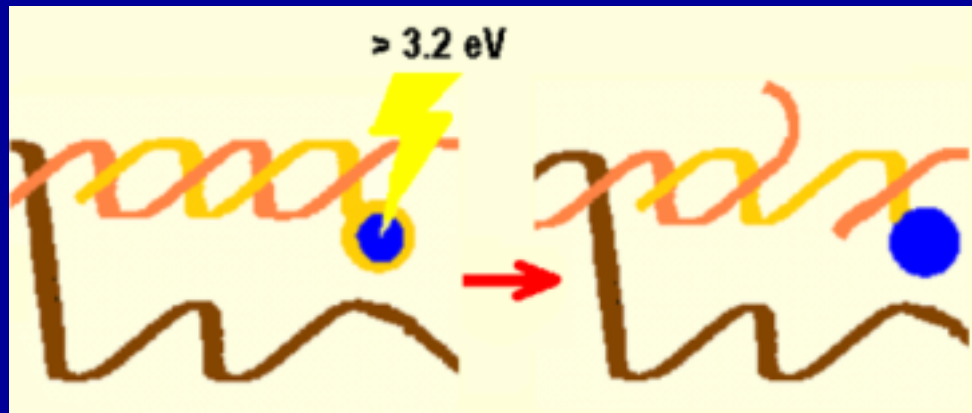
Part I)

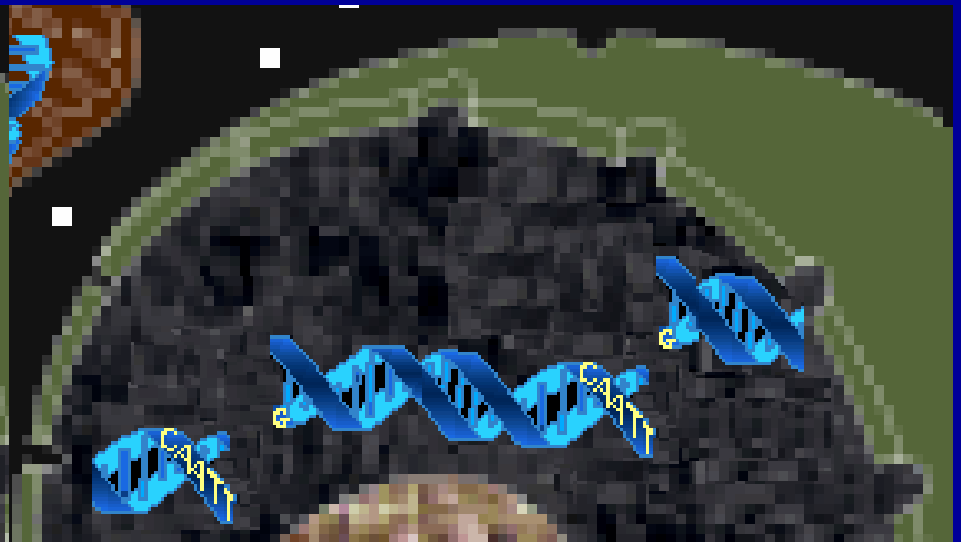
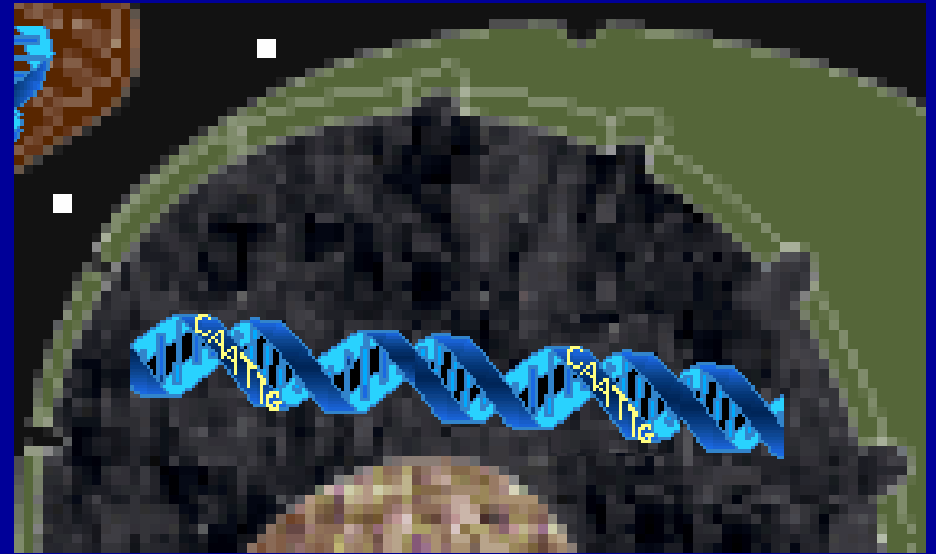
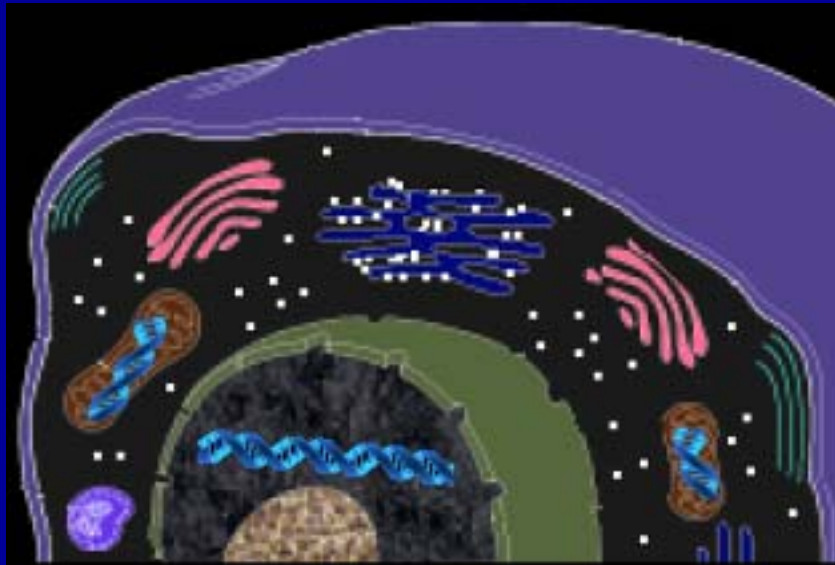
$\text{TiO}_2$  nanocomposites with attached specific DNA sequence should be retained in those locations inside the cell where complementary cellular DNA sequence is located.

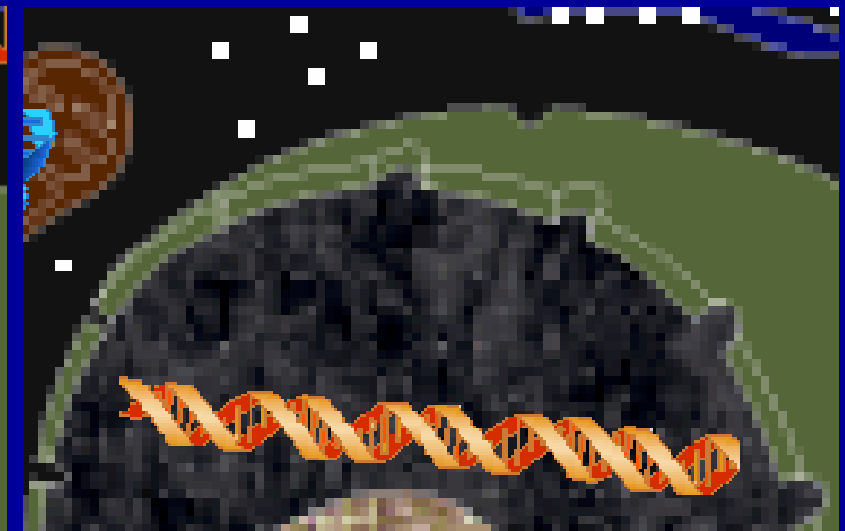
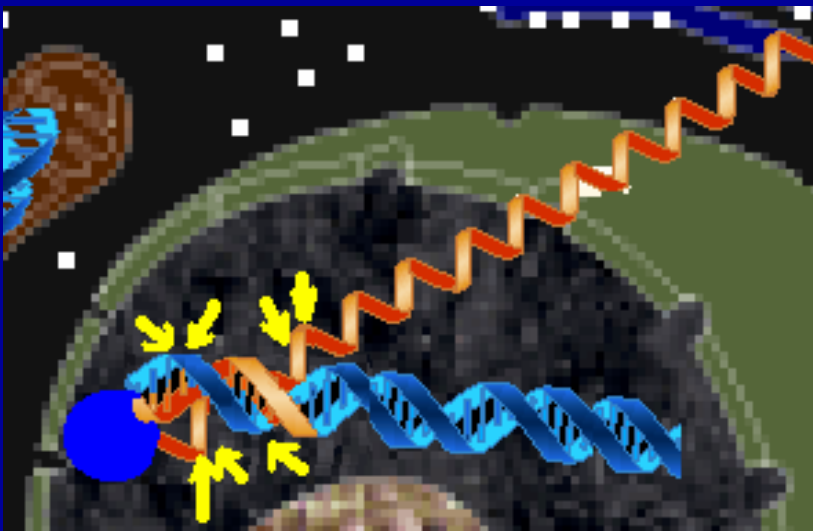
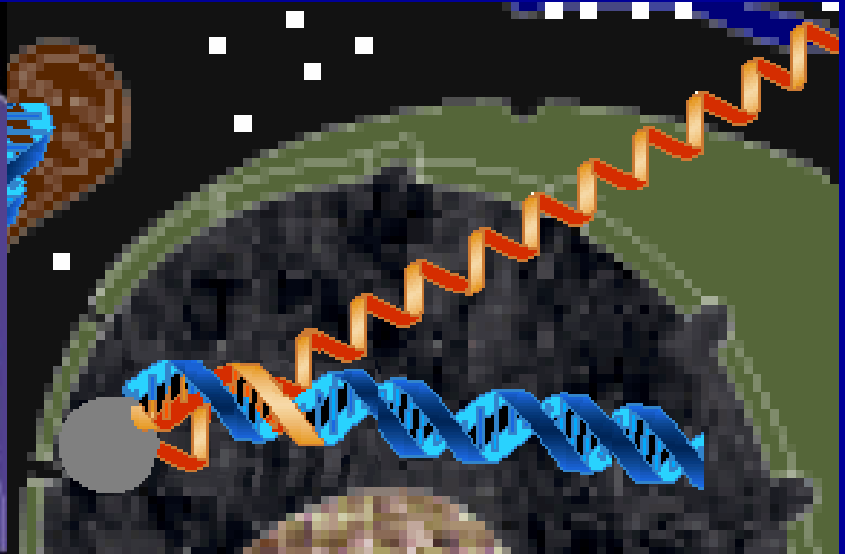
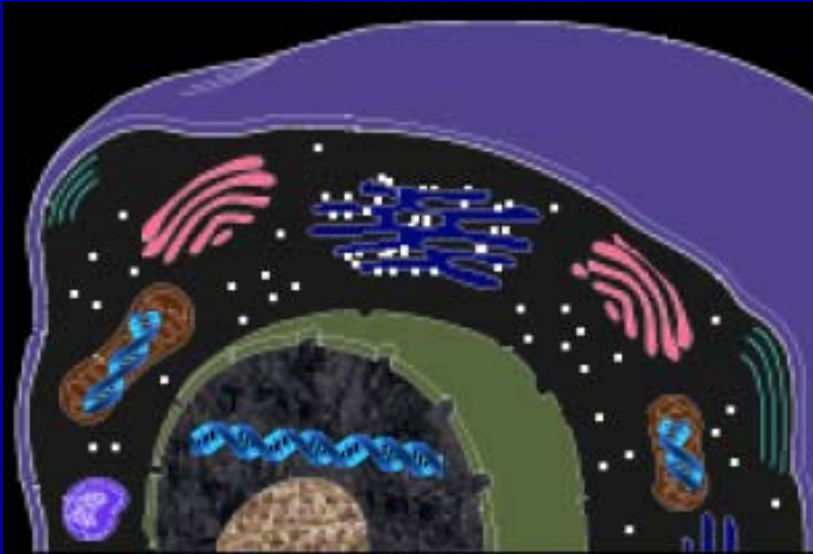


Part II)

Excited  $\text{TiO}_2$  nanocomposites (illuminated by electromagnetic radiation higher than 3.2 eV = white light to gamma-rays) will do charge separation—keeping electrons inside  $\text{TiO}_2$  nanoparticles and releasing electropositive holes onto attached biomolecule—DNA.







## Applications of Biomolecule-Metal Hybrid Nanocomposites

Gene mapping  
Gene sequencing  
Intracellular mapping

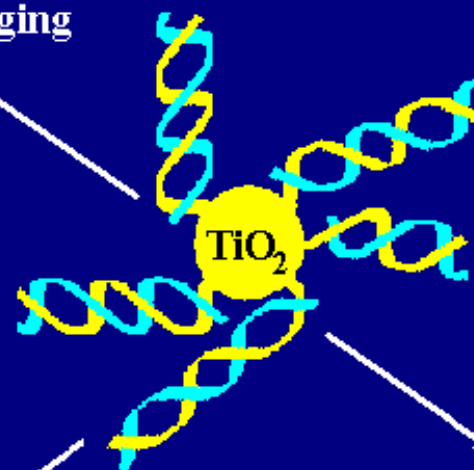
Nanomolecular tagging

**INFORMATICS**

**STRUCTURE**

Nanoscaffolds

Structural studies of biomolecular assemblies



**MANIPULATION OF FUNCTION**

Multifunctional nanomachines

Intracellular manipulation  
Gene therapy  
Biosensors

**Northwestern University/Argonne National  
Laboratory Biology:**

**Gayle E. Woloschak  
Tatjana Paunesku  
Nataša Stojićević  
Miroslava Protić**

**Argonne National Laboratory Chemistry:**

**Tijana Rajh  
Marion Thurnauer**

**Argonne National Laboratory Advanced Photon  
Source XOR-CAT:**

**Jörg Maser  
Stefan Vogt  
Barry Lai**